

**IMECE2008-68796**

## COMPLIANT IMPACT GENERATOR FOR REQUIRED IMPACT AND CONTACT FORCE

**Burak DEMİREL**  
Graduate Student  
ME Department,  
İstanbul Technical University.  
İstanbul, Turkey  
[demirelbu@itu.edu.tr](mailto:demirelbu@itu.edu.tr)

**Mümin Tolga EMİRLER**  
Graduate Student  
ME Department,  
İstanbul Technical University.  
İstanbul, Turkey  
[emirler@itu.edu.tr](mailto:emirler@itu.edu.tr)

**Ahmet YÖRÜKOĞLU**  
Graduate Student  
ME Department,  
İstanbul Technical University.  
İstanbul, Turkey  
[ahmetyorukoglu84@yahoo.com](mailto:ahmetyorukoglu84@yahoo.com)

**Nebahat KOCA**  
Graduate Student  
ME Department,  
İstanbul Technical University.  
İstanbul, Turkey  
[nebahat.koca@gmail.com](mailto:nebahat.koca@gmail.com)

**Ümit SÖNMEZ\***  
Assistant Professor  
ME Dept. MEKAR Laboratory  
İstanbul Technical University.  
İstanbul, Turkey  
*\*Corresponding Author*  
[usonitu@gmail.com](mailto:usonitu@gmail.com)

### ABSTRACT

A novel design of compliant slider crank mechanism is introduced and utilized as an impact force generator and contact force generator. This class of compliant slider mechanisms incorporates an elastic coupler which is an initially straight flexible beam and buckles when it hits the stopper. The elastic pin-pin coupler (a buckling beam) behaves as a rigid body prior to the impact pushing the rigid slider. At a certain crank angle the slider hits a stopper generating an impact force. Impact force can be changed by changing the angular velocity of the crank, therefore; achieving a desired velocity of the slider. Moreover, after the impact when the vibrations die out the maximum contact force can also be predetermined by designing the coupler dimensions (length, width, thickness and the amount of compression). Contact duration (crank angle) can also be changed and adjusted in this mechanism by changing the adjustable location of the impacted object.

### NOMENCLATURE

$R_1$	Ground link length
$R_2$	Crank length
$R_3$	Flexible link length

$\theta_1$	Ground link orientation
$\theta_2$	Crank angle
$\theta_3$	Flexible link angle
$w_2$	Angular velocity of crank
$w_3$	Angular velocity of flexible link
$I_e$	Coefficient of restitution
$F_r$	Contact force during the restoration
$F_d$	Contact force during the deformation
$v$	Velocity
$L_{orig}$	Length of flexible beam before buckling
$L_{beam}(\theta_2)$	Length of flexible beam after buckling
$U$	Flexible beam deflection
$u$	Normalized deflection
$E$	Displacement between the crank joint and stopper
$\phi$	Applied complementary force angle with the horizontal
$\theta_{2cr}$	Crank angle when the slider hits the stopper
$EI$	Flexible beam's elastic rigidity
$F_{pin-pin}$	Buckling beam force
$F_{contact}$	Contact force
$p(u)$	Normalized load

## INTRODUCTION

Compliant mechanisms include at least one flexible member with rigid links. Compliant mechanisms are made from elastic elements which deflect to accomplish a required motion.

Compliant mechanisms transfer an input force or displacement to another point by utilizing their elastic body deformation (1). The motion of the mechanism is partially or completely produced by the elasticity of its links beside the mobility provided by its more conventional rigid body counterparts.

The concept of compliant of flexible mechanism is not new (2). However, the compliant mechanisms are well-suited for MEMS, have received increasing attention recently because of its superior properties and suitability for micro manufacturing.

The compliant mechanisms have many advantages over to the conventional rigid-body mechanisms. These advantages can be classified in two categories:

- The cost reduction
- The increased performance.

In the first category; decreased assembly time, simplified manufacturing processes, and requiring fewer parts can be counted. In the second category; increased precision due to reduced number of joints, accuracy, less wear, reduced weight and friction, decreased built-in restoring force can be counted. Compliant mechanisms also have fewer movable joints which result in less wear and have no need for lubrication (2, 5, 6, 7 and 8).

In compliant mechanisms energy is stored in the form of strain energy due to the deflection of flexible members. This form of potential energy in some cases is stored in the whole body where the compliance is distributed. However; in some applications, stored energy in flexible members can be disadvantageous where uncontrolled transform of the strain energy to the kinetic energy occurs.

On the other hand this sudden energy released and storage can be utilized for beneficial purposes. This aspect helps to broaden the range of the compliant mechanism design. Force deflection feature and the stored strain energy deflection feature of the flexible members may be taken into account for beneficial purposes (5).

The compliant mechanisms allow the designer greater freedom in the number of possible solutions. Nevertheless, the compliant mechanism design freedom is usually compensated the difficulties in the analysis of the compliant mechanism members.

Generally, the compliant mechanism analysis is geometrically nonlinear due large bending/deflections of its flexible elements.

When the elastic deflections are large enough in the nonlinear range, the dynamic analysis is going to be quite complicated.

The dynamic response of the compliant mechanism comparing to the quasi-static response of the mechanism can be quite different and the mechanism's dynamic response can not be ignored (3, 4).

In order to synthesize the compliant mechanisms dynamically, usually the simulation of the mechanism should be done for several different variables due to the difficulties to synthesize the mechanism considering the complexity of the dynamic analysis.

In the mechanism's world, the slider crank mechanism is one of the most common ones. This is the easiest mechanisms to analyze because its links form of a triangle. The slider crank mechanism is known by converting a rotational motion into a linear motion.

The steady state solutions of the slider crank mechanism have been studied by Jasinski et al. (9), Zhu and Chen (10) and Badlani et al. (11).

The velocity control of the slider crank mechanism's typical application is found in petrol and diesel engines. This aspect is also covered numerically by changing the angular velocity of the novel compliant slider crank mechanism introduced in this research.

The object of this investigation is to model the dynamic behavior of the compliant crank slider mechanism which is utilized as a required impact generator and contact force generator.

The mechanisms that are called constant force mechanisms (12) generate reaction force at the output part of the mechanism which does not change for great range of the input part. Constant force generating applied to a surface may be useful in many applications. The concept behind this project is somewhat similar (a required force application concept is the same as the constant force mechanism) to the compliant constant force mechanism *but the general idea of generating a required impact force and contact force is unique.*

In our design project, the compliant crank slider system incorporates an elastic coupler beam connected to the rigid crank. The flexible pin-pin coupler behaves as rigid body prior to impact pushing the rigid slider. The impact force can be determined and changed by the adjusting of the angular velocity of crank. The reciprocal motion of the slider can be obtained in terms of the crank motion.

The angular velocity of the crank is changed for different runs this determines the velocity of the slider; therefore the impact force can be adjusted.

Moreover, after the impact when the vibrations settle the maximum contact force can be adjusted by designing the flexible beam dimensions and the deflections of the buckled beam. Contact duration can be changed and controlled by two possible ways:

- First the crank angle range during the contact can also be adjusted by the changing the fixed location of the impacted object.

- Second the contact duration can also be adjusted (lengthened or shortened) by changing the crank angular velocity.

This project presents a new concept of using compliant mechanism as an impact force generator and contact generator, a compliant slider crank mechanism with a pin-pin buckling flexible beam coupler is utilized for this purpose. The compliant slider crank mechanism in literature has flexible bending couplers which behaves always elastic, on the hand the coupler of the mechanism presented in this research behaves as a rigid body prior to impact. Compliant mechanism synthesis will be investigated in three parts:

- Rigid body mechanism synthesis prior to impact.
- Formulation of impact forces.
- Calculation of the contact force, after the slider vibrations is stopped and continuous contact is established.

A dynamic model considering the above cases is developed and then simulated. The simulation results are compared with the prototype experimental test results. Outcome from the modeling and testing are discussed in the next section and followed by the conclusions of this work.

## THEORETICAL ANALYSIS

There are several ways to perform kinematic analysis including; graphical, analytical, or simply using commercially available software packages. Graphical methods are helpful to obtain a fast and efficient solution for a particular position. Analytical methods are useful to obtain the simulation of the system for the whole range of the motion. Software packages are powerful tools for analysis and design purposes.

Both vector loop closures and closed form solutions are used for the kinematic position analysis of slider-crank mechanism. The velocity and the acceleration analysis of the mechanism then may be obtained by differentiating position solution with the respect to time (13).

The compliant impact and contact force generator introduced in this project works in the three different modes as explained below:

- In the first working mode before the impact, the flexible buckling link behaves as a rigid body pushes the slider which results in a common slider crank mechanism. A kinematic analysis is performed for this part
- In the second working mode slider hits the stopper; then the flexible beam buckles. The linear momentum linear impulse equations are used to obtain the impact force. The magnitude of the impulse force can be adjusted by changing the angular velocity of the crank and obtaining a desired slider velocity. A dynamic analysis is performed until the slider comes into a stop.
- The third working mode starts after the

vibrations of the slider dies out and continuous contact is established. During the continuous contact flexible link applies a variable contact force. This force increases until the crank reaches a certain angle, then a relaxation of the flexible beam will occur, the contact force decreases steadily after that the contact ends buckling beam returns to the original rigid body position, the first working mode starts again. In order to calculate the contact force history a quasi static analysis is performed in this part.

The equations concerning to these three different modes are stitched together to obtain full simulation of the system during the complete crank rotation.

The kinematic diagram of the compliant impact and contact force generator is shown in fig. 1 before the slider hits the stopper.

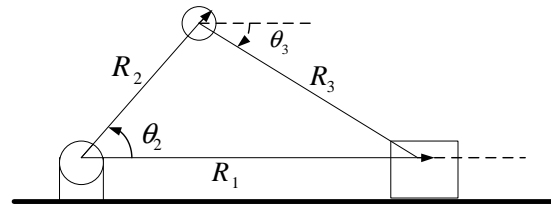


Fig. 1: Slider-crank Mechanism

In order to perform the kinematic analysis of the slider crank mechanism for the first working mode, the well known loop closure equations may be written as,

$$\vec{R}_2 + \vec{R}_3 = \vec{R}_1 \quad (1)$$

The horizontal and vertical components of the loop closure equation are given below;

$$r_2 \cos \theta_2 + r_3 \cos \theta_3 = r_1 \quad (2)$$

$$r_2 \sin \theta_2 + r_3 \sin \theta_3 = 0 \quad (3)$$

Taking the first derivatives of position analysis with respect to time, the following relations for the velocity could be obtained,

$$-r_2 w_2 \sin \theta_2 - r_3 w_3 \sin \theta_3 = \dot{r}_1 \quad (4)$$

$$r_2 w_2 \cos \theta_2 + r_3 w_3 \cos \theta_3 = 0 \quad (5)$$

When the crank angle reaches to a certain angle the impact phenomena will occur which causes the flexible beam to buckle. The impact force can be adjusted by changing the velocity of the slider. By using the linear momentum linear

impulse relationship, the coefficient of restitution  $I_e$  may be written as,

$$I_e = \frac{\int_{t'}^{t''} F_r dt}{\int_{t_o}^{t'} F_d dt} = \frac{m(v_1' - v_o)}{m(v_o - v_1)} = \frac{v_1' - v_o}{v_o - v_1} \quad (6)$$

Impact phenomena are always accompanied by energy loss which may be calculated by subtracting the kinetic energy of the system just after the impact from that of the just before impact. According to classical impact theory; the value of coefficient restitution lies between  $0 < I_e < 1$ . In this project the collision is occurred between wood and wood surfaces, therefore the coefficient of restitution is taken 0.8.

When the pin-pin flexible beam deflects, a nonlinear force which is a function of the deflection is applied to the slider. This buckling force may be calculated considering the pinned-pinned end conditions of the flexible beam using the Elastica theory. A polynomial fit function (6) to the exact large deflection analysis of the flexible pinned-pinned buckling beams is used in this research. In order to acquire the solution of the system; the polynomial fit to the nonlinear Elastica theory, nonlinear algebraic/transcendental equations are used to study the kinematic simulation just before impact and after the contact ends. During the impact linear impulse and linear momentum equations are used until the vibration of the slider dies out due to impact and coulomb friction energy loss.

In fig. 2; the kinematic diagram of the mechanism considering the initial contact angle at the beginning of the impact is represented with the solid line, and the kinematic diagram considering the buckling beam motion is represented with the dashed line.

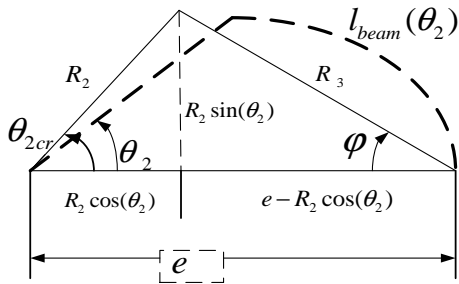


**Fig. 2:** The kinematic diagram of the compliant slider-crank mechanism at two positions

In fig.2,  $\varphi = 180^\circ - \theta_3$  is the  $R_3$  angle with the horizontal,  $\theta_{2cr}$  is the certain angle where initial contact establishes,  $e$  is the distance between the crank joint and stopper. The undeflected length (the original length) of the flexible beam may be written as;

$$L_{orig} = L_{beam}(\theta_2) + U \quad (7)$$

Where  $l_{beam}$  represents the deflected length and  $U$  represents the flexible beam deflection

$$L_{beam}(\theta_2) = \sqrt{((R_2 \sin \theta_2)^2 + (e - R_2 \cos \theta_2)^2)} \quad (8)$$

From the geometrical analysis of the mechanism (see fig. 2), the deflection of the flexible beam  $U$  can be expressed as;

$$U = L_{orig} - \sqrt{((R_2 \sin \theta_2)^2 + (e - R_2 \cos \theta_2)^2)} \quad (9)$$

The complementary contact angle  $\varphi$  can be found as,

$$\varphi = \arctan\left(\frac{R_2 \sin(\theta_2)}{e - R_2 \cos(\theta_2)}\right) \quad (10)$$

When the flexible beam buckles, it applies a nonlinear force function to the slider. The flexible pinned-pinned coupler is a two force member and its normalized deflection is calculated from the Elastica theory. A polynomial curve fit plot is shown in fig. 3 and the corresponding normalized equation is given below; the reader should refer to (14) for detailed analysis.

$$p(u) = 7.1908239u^4 - 6.2016131u^3 + 6.253177u^2 + 4.3898032u + 9.8879488 \quad (11)$$

Where  $p$  and  $u$  represents the normalized deflection  $u = U/L$  and the normalized load  $p = PL^2/EI$ .

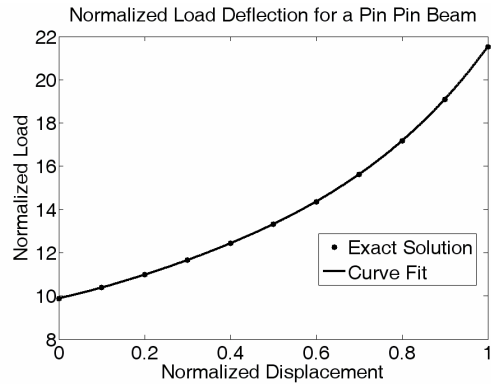


**Fig. 3:** Normalized load versus normalized displacement

The schematic of the mechanism's stopper is shown below (see fig. 4) during the contact. While applying the linear momentum linear impulse relationships; flexible beam force and flexible angle is assumed to be constant (their change is insignificant for the crank speed considered in this research; the slider jumps back for very short distance). The impulse

momentum equations are applied until the slider stops at the contact point.

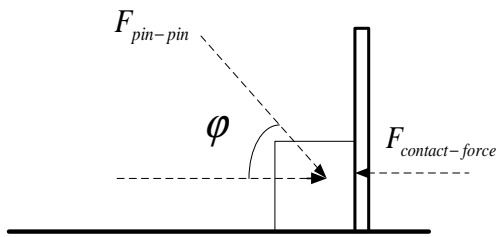


**Fig. 4:** The slider generates a contact-force

After the slider comes to a stop the following equations are applied to calculate the contact force.

$$F_{pin-pin} = \frac{p(u)EI}{L_{beam}^2} \quad (12)$$

$$F_{contact} = F_{pin-pin} \cos(\phi) \quad (13)$$

### SIMULATION RESULTS

The equations 1-12 are used to obtain numeric simulation results of the compliant slider crank mechanism impacting to a stopper. The simulation block diagram method is used in MATLAB and Simulink to solve these Equations 1-12. The simulation block diagram of the mechatronic system consists of three subsystems. In the first subsystem, the kinematic analysis of the slider crank mechanism is included. In the second subsystem, the impact force is calculated using the linear momentum, linear impulse equations. In the third subsystem, the contact force is calculated by using polynomial fits to exact Elastica solution. These three sets of subsystems are stitched together using if statements.

The simulation result of the mechanism is presented in Fig. 5 for a constant angular velocity (1.25 rad/sec). The impact force is approximately 27 Newton as seen from the Fig. 5 and the period of the movement of the slider is 5 seconds for one revolution.

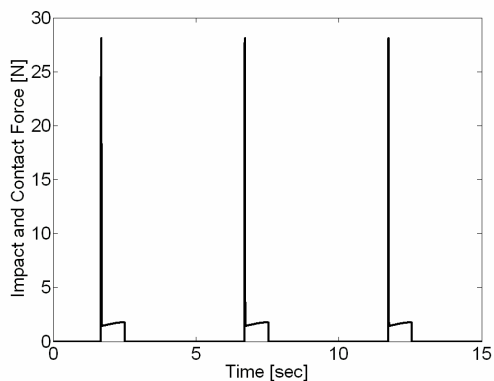


**Fig. 5:** The magnitude of the impulse and contact force for constant angular velocity

The magnitude of the impact force can be adjusted by changing the slider's velocity. The impact and contact force graphic is shown in fig. 6 for the ramp input. The input angular velocity changes linearly 0.75 - 6.58 rad/sec. The magnitude of the impulse force increases when the input voltage of system increases. Moreover, the period of the impulses decreases as a result the angular velocity of the crank increases. However, it is easily seen that the duration time of the contact force decreases when the angular velocity of the crank rises.

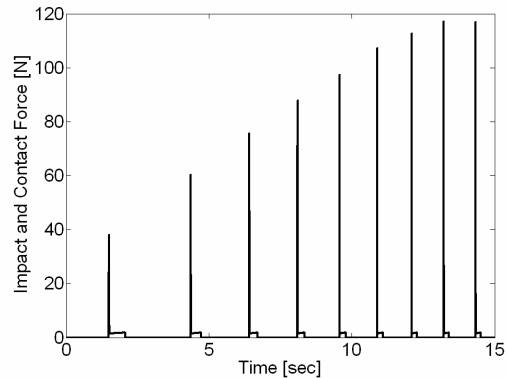


**Fig. 6:** The magnitude of the impulse and contact force for ramp angular velocity

### EXPERIMENTAL SETUP

Experimental setup is described at this section. Figure 7 and Figure 8 show a picture of the compliant slider crank mechanism prototype and a schematic of it respectively. This prototype is used to validate the conceptual contributions of the project. The mechanism is composed of a slider, a crank and a flexible beam mainly.

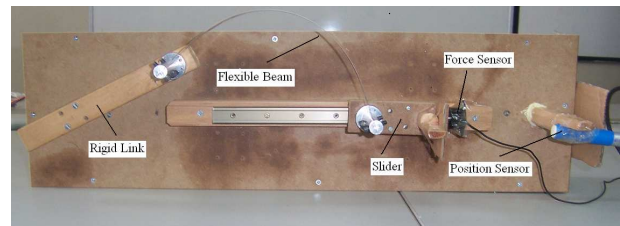


**Fig. 7:** The compliant slider crank prototype mechanism

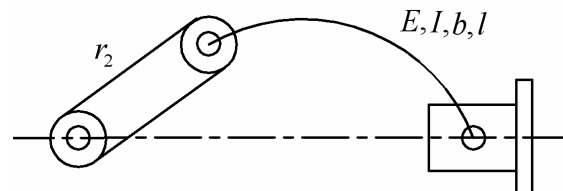


**Fig. 8:** Schematics of the slider crank mechanism

Test mechanisms dimensions and related parameters are listed in tab. 1.  $E$  is the modulus of elasticity. The variables;

$b$ ,  $h$  and  $I$  are flexible beam's width, thickness, and moment of area respectively.

**Tab. 1:** The slider crank mechanism dimensions

Parameter	Value
$r_2$	140 mm
$r_3$	310 mm
$E$	$210 \times 10^9$ MPa
$b$	30 mm
$h$	0.3 mm
$I$	$0.0675 \text{ mm}^4$

Before running dynamic simulations using the values in tab. 1; how to obtain different maximum contact force is explained in this paragraph. The affect of contact force generated by this novel mechanism depends on the dimension of the pinned-pinned buckling beam. Table 2 shows the magnitude of the maximum contact force (at the location of the maximum deflection) which can be generated for three different in plane thicknesses of the flexible beam (the other dimensions are the same: Namely the length and out of plane width). The maximum contact force generated by using the buckling beam whose thickness is 0.3 mm is 27 times and the maximum contact force generated by using buckling beam whose thickness is 0.5 mm is 125 times bigger than that of the 0.1 mm beam. The maximum contact force is rising with the cubic power of the thickness of the flexible beam due to the fact that the second moment of area depends on the cubic power of the thickness for rectangular cross sections.

**Tab. 2:** The Properties of Flexible Link

Thickness of beam	Maximum Contact Force
0.1 mm	0.0655 N
0.3 mm	1.7684 N
0.5 mm	8.1871 N

The experimental setup was constructed to allow testing for different motor angular velocities. DC motor is used with gear-box to increase the torque of the motor. Two sensors are incorporated into the mechanical set up for measuring the position of the slider and the force generated by the impact and the contact. For position measurements, an ultrasonic position sensor is used. The ultrasonic position sensor is mounted behind the stopper. Moreover, a force sensor is used to measure force exerted on the slider which measures the forces up to 44.18N.

The data from the measurements of the impact forces, contact forces and also positions are acquired with IOtech personal DAC 3000 series data acquisition card. Data processing is performed by MATLAB/SIMULINK software package.

The working principle of the mechanism is different from that of the conventional slider crank mechanism. This mechanism behaves in two different modes: the rigid mode and the flexible mode. The rigid mode of the mechanism is shown in fig. 9 and the flexible mode is shown previously in fig. 7 respectively.

At the crank angle range of between  $120^\circ$  and  $180^\circ$ ; the mechanism behaves like the flexible slider crank. When the crank angle reaches  $120^\circ$ , the slider hits the stopper and the system generates an impact force applied to the stopper. After the vibrations stops until the crank angle reaches  $180^\circ$ , a contact force is formed by the slider applied to the stopper.

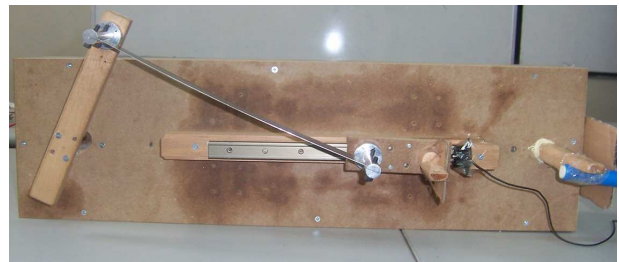


**Fig. 9:** The rigid mode of the slider crank mechanism

For the other crank angle locations, the compliant mechanism behaves like a rigid slider crank mechanism. The magnitude of the impact force, contact force and the contact time can be adjusted by changing the angular velocity of the actuator (dc motor). The crank angular velocity is regulated by changing the input voltage of the dc motor. This system starts to work near 2.5 V input voltage and continues to generate required impact and contact force up to the 4.5V input voltage (above this voltage the force sensor output is of the scale).

## EXPERIMENTAL RESULTS

Experimental results are obtained for different voltages of the DC motor therefore the effects of the voltage on the generated force (impact force) can be seen. The results are obtained for DC motor voltage 2.5V and 3V.

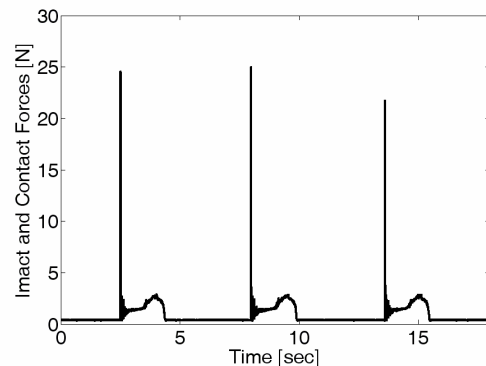


**Fig. 10:** Impact and contact forces versus time (motor voltage 2.5V)

The alterations/changes of impact force and the somehow identical contact forces (they are not exactly the same, because the angular velocity is different but the maximum magnitude and the profile is the same) versus time can be observed from the fig. 10 and fig. 11. When the motor voltage is 2.5 Volt, the impact force reaches approximately 25 N. If the motor voltage is raised to 3 Volt; the impact force reaches approximately to 30 N. In both fig. 10 and fig. 11, the similar contact force history caused by buckled the flexible beam can be observed.

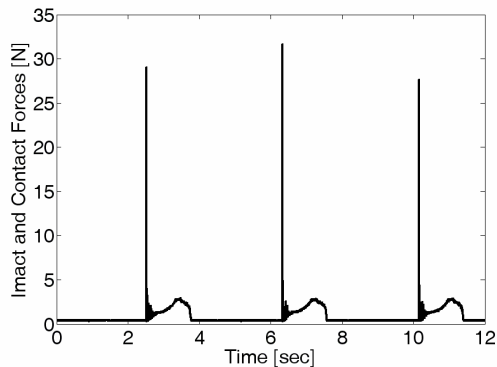


**Fig. 11:** Impact and contact forces versus time (motor voltage 3V)

## CONCLUSIONS

This paper presents a brief background of compliant crank slider mechanism used as a compliant impact generator for a required impact and contact force. The kinematic and the dynamic analysis have been used to designate the motion characteristic for slider-crank mechanism. The prototype proved the conceptual approach behind the design of the compliant impact and force generator mechanism. Different impact forces are obtained by changing the crank angular velocity experimentally and numerically. In this mechanism; the slider attached to the crank with a flexible beam. The flexible beam acts as a rigid body and does not buckle until the certain angle is reached (when the slider hits the stopper). After reaching this angle the flexible beam begins to buckle and it applies increasing force to the impacted object. In experimental setup; the impact force data of the mechanism has been collected and compared with the force analysis of the mechanism.

## ACKNOWLEDGMENTS

This research is supported through the Ümit Sönmez's Career Award 2005 105M191 by Turkish Scientific and Technological Research Council (TÜBİTAK), and it is based on the term project assigned in Modeling of Mechatronic Systems Class in Istanbul Technical University.

## REFERENCES

[1] Howell L. L., Midha A., and Norton T. W., 2000, "Limit Positions of Compliant Mechanisms Using the Pseudo-Rigid-Body Model Concept," *Mechanism and Machine Theory* 35 (2000) 99-115.

[2] Her I., and Midha A., 1987, "A Compliance Number Concept for Compliant Mechanisms and Type Synthesis," *Journal of Mechanisms, Transmissions and Automation in Design*, Transactions of the ASME 109(3): 348-355.

[3] Parkinson, B. M., Jenson, B. D., and Roach, G. M., 2000, "Optimization-Based Design of a Fully-Compliant Bistable Micro Mechanism," *Proceedings of 2000 ASME Design Engineering Technical Conferences*, DETC2000/MECH-14119.

[4] Masters, N. D., and Howell, L. L., 2003, "A Self-Retracting Fully-Compliant Bistable Micromechanism," *J. of Microelectromech. Syst.*, 12, pp. 273-280.

[5] Howell, L. L., 2001, *Compliant Mechanisms*, Wiley, New York.

[6] Sönmez, Ü., 2007, "Introduction to Compliant Long Dwell Mechanism Designs Using Buckling Beams and Arcs", *ASME J. Mech. Des.*, Vol. 129 pp. 831-843.

[7] N.M. Sevak, and C. W. McLarnan, 1974, "Optimal Synthesis of Flexible Link Mechanisms with Large Static Deflection," *ASME Paper No. 74-Der-83*.

[8] Howell L.L., and Midha A., 1994, "The Development of Force-Deflection Relationships for Compliant Mechanisms," *ASME Machine Elements Machine Dynamics DE* 1994;71:501-8.

[9] Jasinski P.W., Lee H.C., and Sandor G. N., 1971, "Vibrations of Elastic Connecting Rod of a High-Speed Slider Crank Mechanism," *ASME J. Eng. Ind.*, pp 636-644.

[10] Zhu Z.G., and Chen Y., 1983, "The Stability of the Motion of a Connecting Rod," *J. Mechanisms, Transmissions, Automation Design*, pp. 637-640.

[11] Badlilni M., and Kleinhenz W, 1970, "Dynamic Stability of Elastic Mechanisms," *J. Mechanism Design*, pp. 149-153.

[12] Boyle, C., Howell, L. L., Magleby, S. P., and Evans, M. S., 2003, "Dynamic Modeling of Compliant Constant-Force Compression Mechanisms," *Mech. Mach. Theory*, 38, pp. 1469-1487.

[13] Erdman, A. G., and Sandor, G. N., 1997, "Mechanism Design: Analysis and Synthesis", Vol. 1, 3rd Ed., Prentice Hall, Upper Saddle River, NJ.

[14] Sönmez, Ü, and Tutum, C., "A Compliant Bi-Stable Mechanism Design Incorporating Elastica Buckling Beam Theory and Pseudo Rigid Body Model", *ASME Journal of Mechanical Design*, Vol. 130, April 2008.